Eur. Phys. J. A **42**, 489–493 (2009)
DOI 10.1140/epja/i2009-10794-5

THE EUROPEAN PHYSICAL JOURNAL A

Regular Article – Experimental Physics

Structure of neutron-rich nuclei around the N = 126 closed shell; the yrast structure of $^{205}Au_{126}$ up to spin-parity $I^{\pi} = (19/2^{+})$

Zs. Podolyák[1,a], S.J. Steer[1], S. Pietri[1], M. Górska[2], P.H. Regan[1], D. Rudolph[3], A.B. Garnsworthy[1,4], R. Hoischen[3], J. Gerl[2], H.J. Wollersheim[2], H. Grawe[2], K.H. Maier[5,6], F. Becker[2], P. Bednarczyk[2,5], L. Cáceres[2,7], P. Doornenbal[2,8], H. Geissel[2], J. Grębosz[2,5], A. Kelic[2], I. Kojouharov[2], N. Kurz[2], F. Montes[2], W. Prokopowicz[2], T. Saito[2], H. Schaffner[2], S. Tashenov[2], A. Heinz[4], T. Kurtukian-Nieto[9], G. Benzoni[10], M. Pfützner[11], A. Jungclaus[7], D.L. Balabanski[12], C. Brandau[1], B.A. Brown[13,1], A.M. Bruce[14], W.N. Catford[1], I.J. Cullen[1], Zs. Dombrádi[15], M.E. Estevez[16], W. Gelletly[1], G. Ilie[8], J. Jolie[8], G.A. Jones[1], M. Kmiecik[5], F.G. Kondev[17], R. Krücken[18], S. Lalkovski[14], Z. Liu[1], A. Maj[5], S. Myalski[5], S. Schwertel[18], T. Shizuma[1,19], P.M. Walker[1], E. Werner-Malento[2], and O. Wieland[10]

[1] Department of Physics, University of Surrey, Guildford, GU2 7XH, UK
[2] GSI, Planckstrasse 1, D-64291, Darmstadt, Germany
[3] Department of Physics, Lund University, S-22100, Lund, Sweden
[4] WNSL, Yale University, 272 Whitney Avenue, New Haven, CT, 06520, USA
[5] The Institute of Nuclear Physics, PL-31-342, Kraków, Poland
[6] Department of Physics, University of the West of Scotland, Paisley, PA1 2BE, Scotland
[7] Departmento de Fisica Teórica, Universidad Autonoma de Madrid, Madrid, Spain
[8] IKP, Universität zu Köln, D-50937, Köln, Germany
[9] Universidad de Santiago de Compostela, Santiago de Campostela, Spain
[10] INFN, Università degli Studi di Milano, I-20133, Milano, Italy
[11] IEP, Warsaw University, Hoża 69, PL-00-681, Poland
[12] INRNE, Bulgarian Academy of Sciences, BG-1784 Sofia, Bulgaria
[13] NSCL, Michigan State University, East Lansing, MI 48824-1321, USA
[14] School of Environment and Technology, University of Brighton, Brighton, BN2 4GJ, UK
[15] Institute for Nuclear Research, H-4001, Debrecen, Hungary
[16] Instituto de Fisica Corpuscular, Valencia, Spain
[17] Nuclear Engineering Division, Argonne National Laboratory, Argonne, IL-60439, USA
[18] Physik Department E12, Technische Universität München, Garching, Germany
[19] Japan Atomic Energy Agency, Kyoto 619-0215, Japan

Received: 31 December 2008 / Revised: 1 April 2009
Published online: 17 May 2009 –
Communicated by J. Äystö

Abstract. Heavy neutron-rich nuclei have been populated through the relativistic fragmentation of a $^{208}_{82}$Pb beam at $E/A = 1$ GeV on a 2.5 g/cm^2 thick Be target. The synthesised nuclei were selected and identified in-flight using the fragment separator at GSI. Approximately 300 ns after production, the selected nuclei were implanted in an ~ 8 mm thick perspex stopper, positioned at the centre of the RISING γ-ray detector spectrometer array. A previously unreported isomer with a half-life $T_{1/2} = 163(5)$ ns has been observed in the $N = 126$ closed-shell nucleus $^{205}_{79}$Au. Through γ-ray singles and γ-γ coincidence analysis a level scheme was established. The comparison with a shell model calculation tentatively identifies the spin-parity of the excited states, including the isomer itself, which is found to be $I^{\pi} = (19/2^{+})$.

PACS. 29.30.Kv X- and γ-ray spectroscopy – 25.70.Mn Projectile and target fragmentation – 23.35.+g Isomer decay

1 Introduction

Experimental information on the neutron-rich $N \approx 126$ nuclei is scarce. It is particularly difficult to access these nuclei experimentally. They are inaccessible with stable beam/target fusion-evaporation reactions and are too heavy to be populated in fission. Although deep inelastic reactions have been used to access relatively high-spin states in nuclei with a few neutrons more than the most

[a] e-mail: Z.Podolyak@surrey.ac.uk

neutron-rich stable isotopes [1], this technique is limited by a general difficulty in channel selection. Projectile fragmentation at intermediate and relativistic energies has proved to be an efficient and selective way of populating states in nuclei far from the valley of stability [2,3] and is an ideal tool for the study of metastable states in heavy neutron-rich nuclei [3]. The highest sensitivity is achieved with decay (both internal isomeric decay and beta decay) spectroscopy. In this technique the delayed gamma rays are correlated with the individually identified ion, thereby minimising the associated background radiation. Information on the excited states populated in this way can be obtained with only $\sim$ 1000 nuclei produced. In its simplest form the technique is sensitive to isomeric decays with lifetimes between 100 ns and 1 ms. The lower limit comes from the flight-time through the fragment separator, the upper limit is determined by the necessity of correlating delayed gamma rays with the implanted ion. However, shorter lifetimes could also be detected if the decay branch by electron conversion was hindered for specific charge states of the ion [4]. In the case of beta-decay, with the use of an active stopper, the delayed gammas and beta can be correlated with the implantation of the incoming ion over more than 10 s.

The first pioneering isomeric decay experiment following the population of heavy nuclei in fragmentation reaction was performed more than a decade ago [3], with further experiments following [5]. More recently, a set of experiments have been performed at GSI aimed at the study of neutron-rich $N \approx 126$ nuclei.

Studies of magic nuclei are of fundamental importance in our understanding of the nuclear structure since they allow direct tests of the purity of shell model wave functions. Information on the single-particle energies can be derived from the experimental observables such as the energies of the excited states and transition probabilities. The experimental information on the structure of these nuclei can be used as building blocks for calculating more complex configurations. The more information that is available, the more robust are the predictions that can be made on the properties of more neutron-rich species. These are of particular importance as the r-process path nuclei, experimentally unreachable in this mass region so far, are approached [6].

In this contribution new experimental information obtained on the closed $N = 126$ neutron shell nucleus ^{205}Au is presented. The same experiment provided a vast amount of information on a large number of nuclei with $N \leq 126$ [7–10], most notably the yrast structure of the four-proton hole nucleus $^{204}_{78}$Pt was observed up to spin-parity 10^+ [10].

2 Experimental details

Heavy neutron-rich nuclear species were synthesised through the relativistic fragmentation of a ^{208}Pb beam at $E/A = 1$ GeV on a 2.526 g/cm^2 thick Be target. The beam was accelerated using the GSI UNILAC and SIS-18 accelerators; the primary beam intensity was of 9×10^8 particles per spill, with the period between the start of each spill being 25 seconds and the spills lasting for 8 seconds. After exiting the target, the "cocktail" of secondary beam fragments was selected and identified using the GSI FRagment Separator (FRS) [11]. The FRS was operated in achromatic mode with a wedge-shaped degrader in the intermediate focal plane. The identified ions were stopped in an $\sim$ 8 mm thick perspex passive stopper, positioned at the final focal plane of the FRS. The stopper was surrounded by the RISING array in the "Stopped Beam" configuration [12,13]. The details of the experimental setup employed in the present experiment as well as the identification procedure are described in refs. [10,14].

In total nine different magnetic rigidity settings of the FRS were used during the experiment [7,9]; three of these, optimised for the maximum transmission of ^{192}W, ^{199}Os and ^{203}Ir, transmitted ^{205}Au nuclei. The total number of ^{205}Au nuclei implanted in the stopper was $\sim 340 \times 10^3$, with $\sim 240 \times 10^3$ of these ($\sim$ 70%) produced in the setting centred on ^{199}Os.

The identification spectra for the data collected in the ^{199}Os setting are given in fig. 1. The charge state of the ions can be obtained from the energy loss at the final focal plane *vs.* change in magnetic rigidity, $\Delta B\rho$ ($\propto q^2$), at the intermediate focal plane matrix (fig. 1 (top)). To a large extent the ions labelled with $\Delta q = 0$ (those that do not change charge state when passing through the wedge placed in the middle focal point of the FRS) are fully stripped during the whole flight-path from target to stopper. The nuclei labelled with $\Delta q = -1$ are those which pick up an electron in the middle of the FRS, therefore the majority of them are fully stripped in the first part of the separator and H-like in the second half of it. The nuclei labelled with $\Delta q = +1$ are those which lose an electron in the middle of the FRS, therefore they are most likely to be H-like in the first part of the separator. The final identification is given by the matrix of position in the final focal plane *vs.* A/q (fig. 1 (bottom)). The mass-over-charge ratio (A/q) is determined from the measured time of flight in the second part of the FRS and from the tracking of the ions [9,10,15].

3 Results and discussion

The γ-ray data associated with ^{205}Au from all three of the FRS settings mentioned above has been combined. The singles γ-ray spectrum is presented in fig. 2 and details of the transition energies and intensities are given in table 1. Seven transitions are observed, with energies of 243, 737, 928, 946, 962, 980 and 1172 keV. Individual measurements of the decay curves associated with each of the observed transitions have been performed. In all cases the measured half-lives are observed to be identical, within experimental uncertainties. This indicates that all of the transitions are emitted following the decay of a single isomer. The final measured half-life of that isomer is determined by combining the statistics from all of the transitions, with the exception of the 243 keV transition (which is excluded

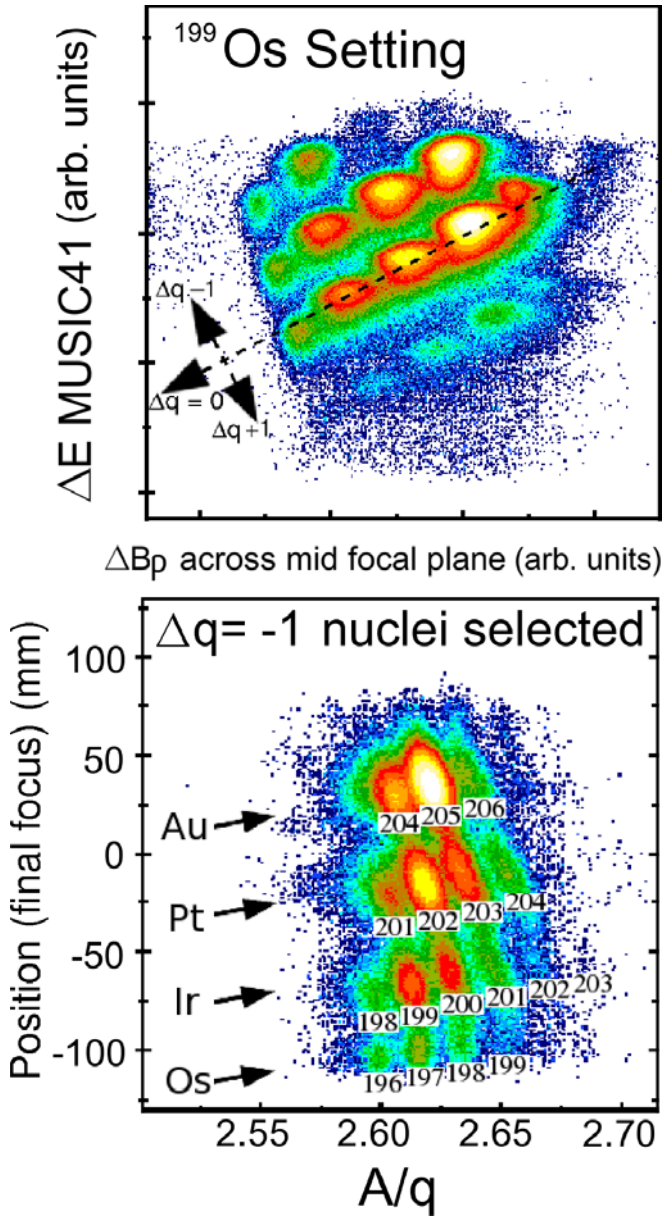

Fig. 1. Identification of the fragmentation products in the FRS setting optimised for ^{199}Os transmission. Top: energy loss at the final focal plane *vs.* change in magnetic rigidity at the intermediate focal plane. This distinguishes between nuclei with different charge states, see text. Bottom: position at the final focal plane *vs.* A/q in the second stage of the FRS for H-like ($\Delta q = -1$) nuclei.

due to its low intensity on a relatively high background). The half-life is found to be $T_{1/2} = 163(5)$ ns.

The statistics obtained allows γ-γ coincidence analysis to be performed. A γ-γ coincidence matrix was built with the conditions that both photons are detected in the time window $\Delta t = 25 \rightarrow 700$ ns following the implantation, and that they are observed within 100 ns from each other. In fig. 3 the relevant gated coincidence spectra are presented.

The energies of the identified γ-ray energies suggest the existence of three parallel decay branches. The 737 + 1172,

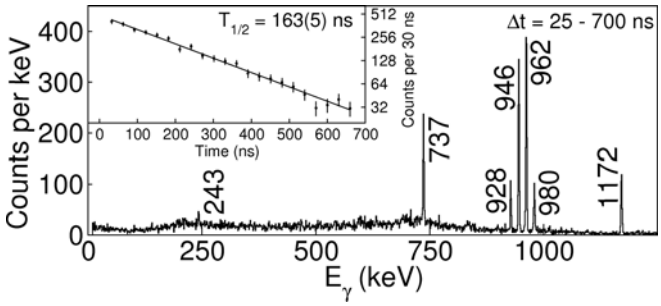

Fig. 2. Singles γ-ray spectrum observed in the time range $\Delta t = 25 \rightarrow 700$ ns following the implantation of nuclei identified as ^{205}Au. Inset: background-subtracted decay curve from the combined statistics of all identified transitions, with the exception of the 243 keV transition; the fit to the data was performed by the least-square method to a single exponential decay.

Table 1. Measured ^{205}Au transition energies and γ-ray intensities. The uncertainty on γ-ray energies is 0.3 keV, except for the 243 keV transition which has an uncertainty of 0.5 keV.

E_γ (keV)	I_γ (arb. units)
243.4	4(2)
736.9	39(2)
928.3	23(2)
946.1	94(4)
962.5	100(5)
962.5	11(4)
980.2	24(2)
1171.5	32(2)

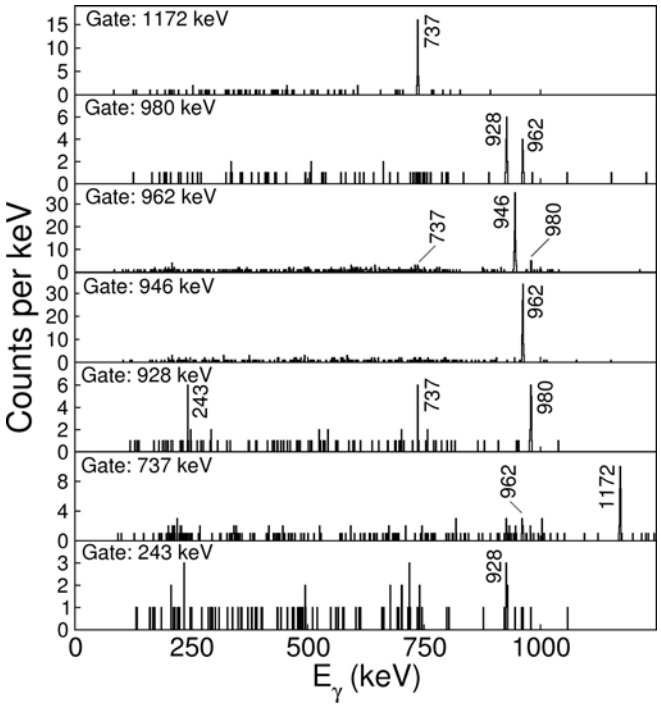

Fig. 3. γ-γ coincidence spectra associated with ^{205}Au. The γ-rays were detected in the time range $\Delta t = 25 \rightarrow 700$ ns following the implantation of the nucleus, with the time difference between the γ-rays being ≤ 100 ns.

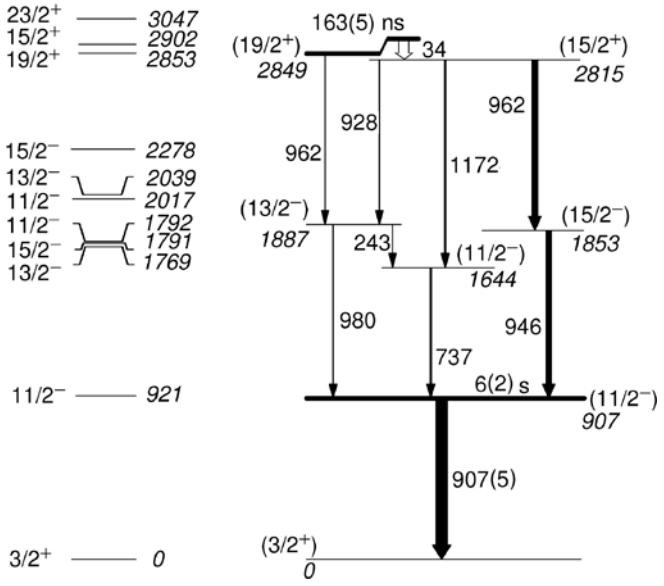

Fig. 4. Left: yrast and near-yrast predicted excited states in ^{205}Au for excitation energies of up to ~ 3 MeV, for details of the shell model calculation, see text. Right: the experimental level scheme obtained in the current work. The energy and the half-life of the first-excited state are from [21]. The spin and parity assignments were obtained from comparison with the shell model calculations.

928 + 980 and the 946 + 962 keV pairs all add up to 1908 keV to within 0.2 keV from one another (see table 1). Also, it is likely that the 243 keV γ-ray connects two of these parallel decay routes, since 980 − 737 = 243. The coincidence analysis supports these conclusions. In addition, it turned out that the 962 keV line is a doublet. It is in coincidence not only with its expected partner 946 keV transition, but also with the 980 keV line. The level scheme constructed is shown in fig. 4. The existence of an unobserved highly converted 34 keV transition had to be inferred from the data.

Shell model calculations for ^{205}Au have been performed in the $s_{1/2}$, $d_{3/2}$, $h_{11/2}$, $d_{5/2}$, $g_{7/2}$ ^{208}Pb proton-hole space with the OXBASH code [16] using single-particle energies obtained from the experimental level scheme of ^{207}Tl [17] and two-body matrix elements (TBME) from ref. [18]. These are based on the Kuo-Brown interaction including core polarisation [19,20], with slight modifications introduced to obtain an improved description of the experimental data available at the time. This parametrisation proved to describe the excited states of ^{206}Hg [1] and ^{204}Pt [10] quite well. The resulting yrast and near-yrast states in ^{205}Au are presented in fig. 4 for excitation energies up to ~ 3 MeV.

^{205}Au is a three proton-hole nucleus, with an expected ground-state configuration of $\pi d_{3/2}^{-1}$ (with the $s_{1/2}$ being empty) and spin-parity $I^\pi = 3/2^+$. The yrast $11/2^-$ state, predicted at 921 keV by the shell model calculations, has $\pi h_{11/2}$ character and it should be long lived since it can decay only through high multipolarity transitions, like in ^{207}Tl [17]. This isomeric state in ^{205}Au was identified in a recent RISING experiment. The K and L conversion electron lines associated to the $11/2^- \rightarrow 3/2^+$ M4 transition were observed. It was found that the $11/2^-$ state has an energy of 907(5) keV and a half-life of 6(2) s [21]. This half-life is much too long to be observed in the present experiment.

Table 2. Measured transition strengths in ^{205}Au compared with those of corresponding transitions in ^{206}Hg [1] and ^{204}Pt [10].

$B(EL)$ (W.u.)	^{205}Au	^{206}Hg	^{204}Pt
$B(E3\colon 19/2^+ \rightarrow 11/2^-)$	0.3(1)		
$B(E3\colon 10^+ \rightarrow 7^-)$		0.25(3)	0.19(3)
$B(E2\colon 19/2^+ \rightarrow 15/2^+)$	1.2(2)		
$B(E2\colon 10^+ \rightarrow 8^-)$		0.94(15)	0.80(8)

The isomeric state observed in the present experiment most probably decays into the $11/2^-$ yrast state. The comparison between the experimental and theoretical level schemes suggests that the isomer has a spin-parity $19/2^+$. Its main decay is via a low energy, 34 keV, $E2$ transition into the yrast $15/2^+$ level. The experimentally deduced transition strength (using the intensities of table 1) is $B(E2) = 1.2(2)$ W.u. We note that our calculations predict the yrast $19/2^+$ and $15/2^+$ states very close in energy, but with the inverse ordering. These states then decay via ~ 1 MeV transitions into the triplet of predicted states at around 1800 keV excitation energy, with spin-parities of $11/2^-$, $13/2^-$ and $15/2^-$. In addition to the low-energy branch, the isomer also has a weaker decay branch, populating the yrast $13/2^-$ state directly via the 962 keV $E3$ transition, with an experimental transition strength of $B(E3) = 0.3(1)$ W.u.

The measured transitions strengths can be compared with those of the corresponding transitions in the neighbouring $N = 126$ nuclei ^{206}Hg and ^{204}Pt (see table 2). The predominant configurations of the $19/2^+$ and $15/2^+$ states in ^{205}Au are $\pi(h^2_{11/2})_{10^+}s_{1/2}$ and $\pi(h^2_{11/2})_{8^+}s_{1/2}$, respectively. The $E2$ transition strength has similar value to those of the analoguos $B(E2\colon \pi(h^2_{11/2})_{10^+} \rightarrow \pi(h^2_{11/2})_{8^+})$ strengths in both ^{206}Hg and ^{204}Pt. The $E3$ transition in ^{205}Au connects the states with main configurations $\pi(h^2_{11/2})_{10^+}s_{1/2}$ and $\pi(h_{11/2}d_{3/2}s_{1/2})$. The corresponding $B(E3)$ transition strengths in both ^{206}Hg and ^{204}Pt are close, although in this case a strict similarity cannot be expected as in ^{205}Au the situation is complicated by the coupling of the $s_{1/2}$ and $d_{3/2}$ protons to 1^+ and 2^+. The measured transition strengths support our interpretation.

4 Conclusions and outlook

Projectile fragmentation when combined with decay spectroscopy is a powerful tool in the study of the structure of exotic nuclei. Several such experiments with the aim of the study of the structure of neutron-rich $N \sim 126$ nuclei

have been performed during the last decade. Here, new experimental information on the closed neutron shell nucleus ^{205}Au was presented. Gamma-ray transitions following the decay of an isomeric state with half-life $T_{1/2} = 163(5)$ ns have been observed and a level scheme was obtained. The spin-parity assignment was performed by comparing the experimental level scheme with shell model calculations.

During recent years a lot of progress has been made in obtaining information on the structure of the heavy neutron-rich nuclei. Recently, measurements using the same technique as presented here, but employing an active Si stopper [22], were performed and information on the β-decay of several nuclei has been obtained [23–25]. Furthermore, nuclei with $N > 126$ and $Z < 82$ were populated in the fragmentation of a ^{238}U beam [26]. The first results from these experiments have just started to emerge. By combining all the experimental information to be obtained from these studies, a much better understanding of this mass region will be achieved.

The excellent work of the GSI accelerator staff is acknowledged. This work is supported by the STFC/EPSRC(UK) and AWE plc. (UK), the EU Access to Large Scale Facilities Programme (EURONS, EU contract 506065), the Swedish Research Council, the Polish Ministry of Science and Higher Education (Grants No. 1 P03B 030 30 and N N202 309135), the Bulgarian Science Fund, the U.S. DOE (Grant No. DE-FG02-91ER-40609), the Spanish Ministerio de Educacion y Ciencia, the German BMBF, the Hungarian Science Foundation and the Italian INFN.

References

1. B. Fornal *et al.*, Phys. Rev. Lett. **87**, 212501 (2001).
2. R. Grzywacz *et al.*, Phys. Lett. B **355**, 439 (1995).
3. M. Pfützner *et al.*, Phys. Lett. B **444**, 32 (1998).
4. M. Caamano *et al.*, Eur. Phys. J. A **23**, 201 (2005).
5. Zs. Podolyák *et al.*, Phys. Lett. B **491**, 225 (2000).
6. H. Grawe, K. Langanke, G. Martinez-Pinedo, Rep. Prog. Phys. **70**, 1525 (2007).
7. S.J. Steer *et al.*, to be published in Int. J. Mod. Phys. E.
8. S.J. Steer *et al.*, in preparation.
9. S.J. Steer, PhD Thesis, University of Surrey, 2008, unpublished.
10. S.J. Steer *et al.*, Phys. Rev. C **78**, 061302(R) (2008).
11. H. Geissel *et al.*, Nucl. Instrum. Methods B **70**, 286 (1992).
12. S. Pietri *et al.*, Nucl. Instrum. Methods B **261**, 1079 (2007).
13. P.H. Regan *et al.*, Nucl. Phys. A **787**, 491c (2007).
14. Zs. Podolyák *et al.*, Eur. Phys. J. ST **150**, 165 (2007).
15. M. Pfützner *et al.*, Phys. Rev. C **65**, 064604 (2002).
16. B.A. Brown, A. Etchegoyen, W.D.M. Rae, The computer code OXBASH, MSU-NSCL report no. 524.
17. D. Eccleshall, M.J.L. Yates, Phys. Lett. **19**, 301 (1965); M.J. Martin, Nucl. Data Sheets **70**, 315 (1993).
18. L. Rydström *et al.*, Nucl. Phys. A **512**, 217 (1990).
19. T.T.S. Kuo, G.H. Herling, Naval Research Laboratory Report 2259 (Washington, DC, 1971).
20. G.H. Herling, T.T.S. Kuo, Nucl. Phys. A **181**, 113 (1972).
21. Zs. Podolyák *et al.*, Phys. Lett. B **672**, 116 (2009).
22. R. Kumar *et al.*, Nucl. Instrum. Methods A **598**, 754 (2009).
23. N. Alkhomashi *et al.*, Acta Phys. Pol. B **40**, 875 (2009).
24. P.H. Regan *et al.*, Int. J. Mod. Phys. E Suppl. **17**, 8 (2008).
25. A.I. Morales *et al.*, Acta Phys. Pol. B **40**, 867 (2009).
26. N. Al-Dahan *et al.*, Acta Phys. Pol. B **40**, 871 (2009).